

## Domain-growth kinetics of Ag on Ge(111)

H. Busch and M. Henzler

*Institut für Festkörperphysik, Universität Hannover, Appelstrasse 2, D-3000 Hannover, Federal Republic of Germany*

(Received 4 April 1989; revised manuscript received 25 September 1989)

The growth of  $\sqrt{3} \times \sqrt{3}$  domains due to Ag on a Ge(111)-(2 $\times$ 4)Ag surface has been studied by spot-profile analysis of low-energy electron diffraction. The exact Lorentzian profile allows an evaluation of the kinetics via the half-width. The domain size grows according to a  $t^{1/2}$  law, indicating a growth mode via movement of domain walls. Measurements at several temperatures provide an activation barrier of 0.52 eV.

### I. INTRODUCTION

Metals on semiconductors have been found to be of widespread interest in the study of interfacial electronic properties.<sup>1,2</sup> They are also of interest with respect to structural aspects, since they form frequently well-defined superstructures, which are, in many cases, much simpler than those complicated structures such as Si(111) 7 $\times$ 7 and Ge(111) 2 $\times$ 8.<sup>3</sup> In recent years imperfect structures have also been of interest. There are a lot of properties which depend inherently on defects (that is, nonperiodic features) like phase transitions, surface diffusion, or surface facetting. Due to the well-defined superstructures and the nearly perfect semiconductor substrates, metals in monolayer quantities on silicon or germanium are ideally suited for careful studies of surface defect phenomena. Whereas the surface-microscopy techniques [such as scanning tunneling microscopy (STM) (Ref. 4) or low-energy electron microscopy LEEM (Ref. 5)] provide excellent qualitative information, quantitative information on size distributions, e.g., is only available after the evaluation of many images which take a long time to be recorded. On the other hand, diffraction techniques immediately provide an average over quite a large area (e.g., 1 mm<sup>2</sup>), they are therefore especially suited for the quantitative analysis of average values, which are needed for a description of thermodynamic and kinetic data.

The kinetics of ordering and the growth of two-dimensional (2D) systems has recently attracted considerable attention.<sup>6-18</sup> Here the form of the growth law and the question of scaling during growth is of interest. Spot-profile analysis of low-energy electron diffraction (SPA-LEED) is especially suited for studying superstructure domains since the profile of superstructure spots depends solely on the domain-size distribution independent of the substrate. There have been studies of the growth of oxygen superstructure domains on tungsten.<sup>16-18</sup> Since a dislocation-free tungsten crystal is not available, all surfaces show terraces with atomic steps, so that ordering only up to 30 nm is observable even with a high-resolution instrument.<sup>17</sup> Semiconductors are usually mosaic-free with a very low density of dislocations, so that kinetic studies are possible for growth up to ordered domains of 200 nm. Metals on semiconductors frequently form well-defined superstructures, which replace the

superstructure of the clean surface. Even growth on top of a superstructure opens many chances by analysis of the spot profile of the superstructure spot of the substrate as demonstrated with Si molecular-beam epitaxy (MBE) on Si(111).<sup>19</sup>

The system Ag on Ge(111) has been chosen, since it fulfills the above requirements in many respects. It shows two well-defined superstructures, the 2 $\times$ 4 structure at  $\Theta=0.25$  monolayer and the  $\sqrt{3} \times \sqrt{3}$  structure for  $\Theta > 0.66$  monolayer.<sup>20,21</sup> For other coverages domains of substrate and/or different adsorbate superstructures are observed. The diffusion of silver on top of the 2 $\times$ 4 structure has been shown to be extremely high,<sup>21</sup> so that ordering phenomena are easily recorded. First experiments with a low-resolution LEED system showed a growth law of  $\sqrt{3} \times \sqrt{3}$  domains with a very low exponent which could not be fit with any theory.<sup>21</sup> Since, due to the low resolution, the deconvolution was an important step in evaluation of the data, the experiments have now been repeated with the newly developed high-resolution LEED instrument.<sup>22</sup> Due to the increase in the resolution by a factor of 10, no deconvolution is needed and the range of measurable half-widths is expanded simultaneously with an increased accuracy. The experiments have been designed to show a clear growth law and a well-resolved spot profile to elucidate the mechanism of growth kinetics.

### II. EXPERIMENTAL

Germanium samples have been oriented and diamond polished to better than 0.2° within the (111) direction. After repeated cycles of sputtering with Ar (beam energy 500 eV) and a short flush for annealing to 800°C a (2 $\times$ 8) LEED pattern was observed with sharp and intense extra spots.

The crystal was mounted between thin tungsten wires which were resistively heated. The temperature of the sample was measured by a Ni-NiCr thermocouple and controlled by feedback within  $\pm 1$  K.

Silver was evaporated from a bead at a hot tungsten wire with a typical rate of about 0.5 monolayers per minute. The crystal was kept at room temperature during evaporation. The evaporated amount was measured with a temperature-controlled quartz crystal balance.

The calibration was derived from the first appearance of the  $\sqrt{3} \times \sqrt{3}$  structure as described in Sec. III A.

All experiments were performed in a standard uHV chamber with a base pressure below  $10^{-10}$  mbar. The profiles of the LEED spots have been recorded by electrostatic scanning with a high-resolution instrument (transfer width 150 nm) (Ref. 22) compared to four grid instruments with about 20 nm resolution.

### III. RESULTS

#### A. Calibration of coverage with extra spot intensities

The clean Ge(111) surface is reconstructed and shows a  $(2 \times 8)$  superstructure. For low silver coverage of about 25% and at substrate temperatures between 150°C and 200°C a  $(2 \times 4)$  superstructure is formed, which disappears at higher coverages to form a  $(\sqrt{3} \times \sqrt{3})R 30^\circ$  superstructure.<sup>20,21</sup>

The integral intensities of extra and normal spots were used for a precision calibration of the coverage. If, by proper heat treatment, the superstructure domains are sufficiently large, LEED intensities increase linearly with coverage until saturation.

For such an analysis a high-resolution LEED (HR-LEED) instrument is especially suited because, even for weak integral intensities, the intensity is well above background, since the peak intensity increases at constant integral intensity with one over the square of the half-width. Therefore, with HR-LEED instruments coverages are also determined precisely where a superstructure just begins to develop.

In Fig. 1 results are presented for a calibration procedure obtained by successive evaporation and annealing. The data are shown for two  $(2 \times 4)$  superstructure spots at energies 59.2 and 72 eV and for one  $\sqrt{3} \times \sqrt{3}$  spot at 59 eV.

Two runs differing in annealing details have been performed, one with 3 min at 420 K, the other with 5–10 min at 480 K, whereas all the measurements have been made at room temperature. While there is no difference for the integral intensities, the  $(2 \times 4)$  peak intensities be-

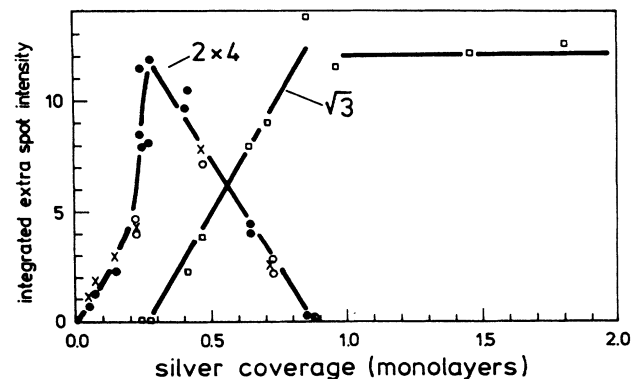


FIG. 1. Integrated intensities of extra spots after deposition of the given amount of Ag and annealing to 420–480 K.

come higher for higher annealing temperatures due to a narrowing of the spot. Here the extra spots have the shape of a threefold asterisk, so that a two-dimensional scan is needed for the determination of the integral intensity.

In contradiction to the assumptions above, the growth of the integral intensities of the  $(2 \times 4)$  is not linear up to  $\frac{1}{4}$  of a monolayer, which may point out the importance of domain boundaries and point defects, so that not all silver atoms are included in well-ordered superstructure domains resulting in background intensity, which is subtracted before integration. For more than  $\frac{1}{4}$  of a monolayer, the decrease of the  $(2 \times 4)$  intensities and the increase of the  $\sqrt{3} \times \sqrt{3}$  intensities is approximately linear. The  $\frac{1}{4}$  monolayer coverage is best defined by the first appearance of  $\sqrt{3} \times \sqrt{3}$  intensity in good agreement with the geometrical arrangement and the calibration of the quartz constants. Independent calibration of the quartz constants has been obtained in Si MBE experiments from monolayer deposition.<sup>23</sup> The saturation coverage for the  $\sqrt{3} \times \sqrt{3}$  superstructure is therefore at  $\Theta = 0.85$  monolayer (ML). This value has also been observed in Auger experiments.<sup>20,21</sup> No further increase in  $\sqrt{3} \times \sqrt{3}$  superstructure intensities was observed. It indicates a further growth only in three-dimensional crystallites, pointing to a Stransky-Krastanov growth, which is also known from silver on silicon.<sup>24</sup>

The saturation coverage of the  $\sqrt{3} \times \sqrt{3}$  superstructure is somewhat striking because the saturation coverage should be a multiple of  $\frac{1}{3}$  of a monolayer. In the Ag/Si(111) system part of the silver was also found to be in  $(1 \times 1)$  domains by STM measurements.<sup>25</sup> A honeycomb model for the  $\sqrt{3} \times \sqrt{3}$  domains takes care of  $\frac{2}{3}$  of a monolayer in an arrangement such as the one found with STM in the Ag/Si(111) system. The rest of the coverage has to be in disordered or in  $1 \times 1$  patches. Several new results are reported in Ref. 2, that, however, do not settle the controversy, if the honeycomb ( $\Theta = \frac{2}{3}$  ML) or trimer models ( $\Theta = 1$  ML) are more likely. For the experiments reported here the difference is not really relevant.

#### B. Growth of $\sqrt{3} \times \sqrt{3}$ domains at saturation coverage

As a starting condition, a well-ordered  $2 \times 4$  structure has always been used. For that purpose a  $\frac{1}{4}$  of a monolayer (or a bit more) has been deposited at room temperature and then annealed at high temperatures (500 K). The extra spots had a half-width of instrumental resolution, so that the perfect single-domain patches had to be at least 200 nm on average. Onto this surface, with exceptional high surface diffusion,<sup>21</sup> silver has been deposited at room temperature. First the amount for the saturation of the  $\sqrt{3} \times \sqrt{3}$  structure has been chosen. Even at room temperature weak and broad  $\sqrt{3} \times \sqrt{3}$  extra spots were visible and the  $2 \times 4$  extra spot intensity was already drastically reduced. For a fast data recording of the  $\sqrt{3} \times \sqrt{3}$  profiles, the energy of  $E = 59.2$  eV was chosen due to the high intensity. Test runs at different energies showed identical profiles at different integral intensities. The  $2 \times 4$  extra spots disappeared immediately during

heating to the temperature where the growth has been measured ( $T > 350$  K).

Spot profiles of a  $\sqrt{3} \times \sqrt{3}$  extra spot have been recorded at a fixed temperature after many time intervals. A decrease of the half-width with time has always been observed, which indicates the growth of domains. For a quantitative description the half-width has been plotted versus the annealing time at a given temperature, both in logarithmic scale in Fig. 2 for a temperature of  $T = 111^\circ\text{C}$ . The plot shows two straight portions. The first one is very accurately described by a growth law with half-width  $h = t^{-x}$  and  $x = 0.5$ , the second one with the smaller slope by  $x \approx 0.25$ . The first two points are off the straight line due to the uncertainty in the definition of the starting time. If one minute is added due to the heating up procedure, those points are again on the straight portion. The special plotting in Fig. 6 avoids the problem (see Sec. III D). All points have been derived from completely recorded profiles. It turned out that all profiles are exactly described by Lorentzians. For demonstration purposes, a set of profiles has been normalized with respect to peak intensity and half-width. As shown in Fig. 3, all profiles are identical within experimental accuracy, although the half-width varies as indicated by a factor of 4 and the peak intensity by nearly 30. The integral intensity as given by the square of the half-width and the peak intensity is nearly constant (variation less than a factor of 2). It shows that domain boundaries and other defects, which do not fit to the  $\sqrt{3} \times \sqrt{3}$  periodicity, have a noticeable, but not important, influence. To show the kind of profile, both a Lorentzian and a Gaussian profile are shown in Fig. 2 with the same normalization. It

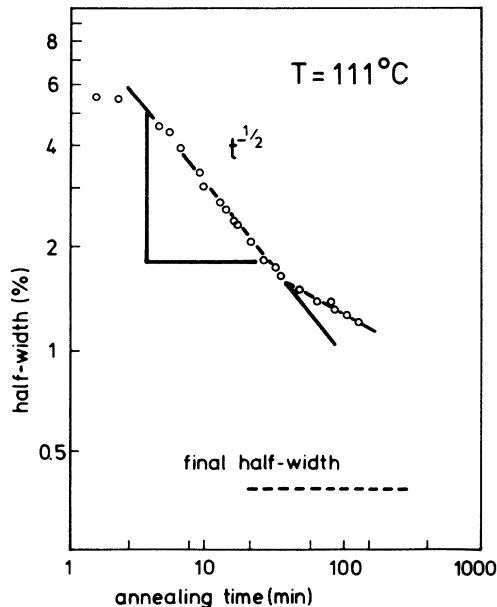


FIG. 2. Half-width (full width at half maximum) of a  $\sqrt{3} \times \sqrt{3}$  superstructure spot after deposition of about  $\frac{2}{3}$  of a monolayer (saturation coverage of  $\sqrt{3} \times \sqrt{3}$ ) on top of a well-annealed  $2 \times 4$  superstructure and annealing at  $111^\circ\text{C}$  for the time given. The final half-width has been obtained after annealing at higher temperatures.

should be noted that the 2D Lorentzian  $I \sim (a^2 + k^2)^{-3/2}$  had to be taken here. It is not possible to describe the profiles by a power law. If, for example, a power of  $-3$  is selected (which fits the outer part of the Lorentzian profile), it would have to be convoluted with the known instrumental response (which has approximately Gaussian shape). Since the half-width of the instrumental response is at least a factor of 5 smaller than the observed half-width, the convolution of any power law and instrumental response is incompatible with the measurement. Only a convolution with a much broader function with variable width would be acceptable. Therefore, the Lorentzian shape is the simplest fit, which describes the changes during growth with a single parameter which may be the half-width as in Fig. 2. To check the accuracy of the exponent  $x$  in Fig. 2, a slope with  $x = 0.45$  has also been tried, with a less satisfying fit. Therefore, the exponent should be  $x = 0.5 \pm 0.05$ . Instead of half-width, frequently the peak intensity is used, especially when the profile cannot be measured accurately over the full Brillouin zone. If all silver atoms are included in the well-ordered atoms, the result should be the same. For comparison, the peak intensity is plotted with the integral intensity in Fig. 4. It is seen that the square root of the peak intensity increases with a power of a bit more than 0.5 due to the slight increase of Ag atoms in the well-ordered domains.

### C. Growth at lower coverage

If less than saturation coverage is deposited onto the well-annealed  $2 \times 4$  structure, the same results are ob-

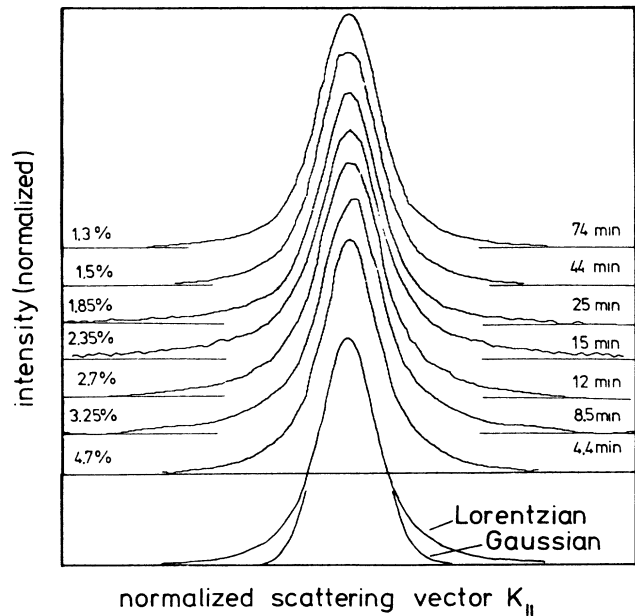


FIG. 3. Spot profiles of the  $\sqrt{3} \times \sqrt{3}$  superstructure spots after different annealing times. For comparison purposes the profiles are normalized with respect to both the maximum and the half-width, so that the perfect agreement with the 2D Lorentzian ( $\frac{3}{2}$  power of the 1D Lorentzian) is demonstrated. The percentages on left-hand side are the half-widths used for scaling.

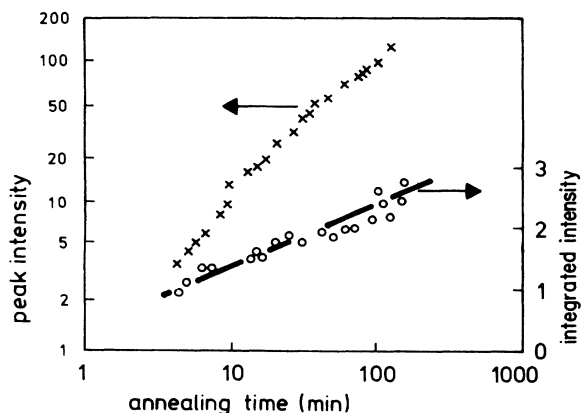


FIG. 4. Peak intensity and integrated intensity of the same measurements as presented in Fig. 2.

served with the difference, that some intensity of the  $2 \times 4$  structure is always observed. The measurements were done at coverages where the  $\sqrt{3} \times \sqrt{3}$  domains covered one-half and three-quarters of the surface. The result for one-half coverage and the same temperature are shown in Fig. 5. It is clearly seen that the steep slope with  $x = 0.5$  ends earlier (20 instead of 30 min) and at a higher half-width (1.9 instead of 1.6%). The second part has, with respect to both half-width and peak intensity, a much lower exponent  $x$ , even in comparison with saturation coverage in Fig. 2.

More information is available from a measurement of the spot profile of an extra spot of the  $2 \times 4$  structure. It consists of a central spike with the half-width of the fully annealed surface ( $2 \times 4$  and  $\sqrt{3} \times \sqrt{3}$  domains of large size, 0.3%) and a shoulder. The intensity of the central spike is given by

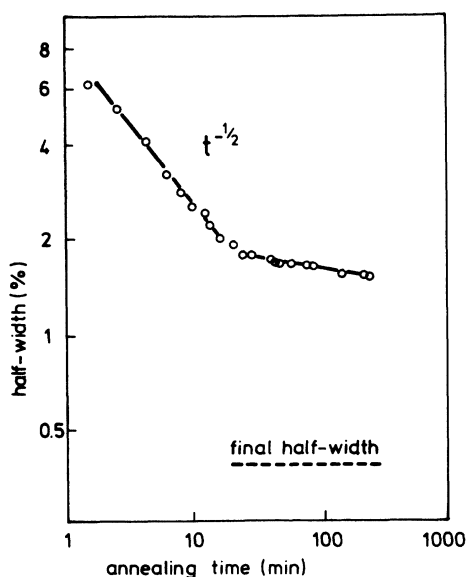


FIG. 5. Half-width of a  $\sqrt{3} \times \sqrt{3}$  superstructure spot vs annealing time. In contrast to Fig. 2, here the  $\sqrt{3} \times \sqrt{3}$  domains cover only about half the surface.

$$I = I_0 \Theta_{2 \times 4}^2,$$

with  $I_0$  the intensity of the extra spot at full coverage with  $2 \times 4$  and  $\Theta_{2 \times 4}$  the remaining coverage of the  $2 \times 4$  structure after the forming of the  $\sqrt{3} \times \sqrt{3}$  domains. Since  $I/I_0 \approx \frac{1}{6}$ , the coverage  $\Theta_{2 \times 4}$  is approximately 0.4, which fits approximately to the measured total coverage  $\Theta_{Ag} = 0.53$ . From Fig. 1 a total coverage of 0.6 is predicted, the difference again is due to disorder at domain edges. During annealing, the shoulder of the  $2 \times 4$  extra spot nearly does not change, although the half-width of the  $\sqrt{3} \times \sqrt{3}$  spot decreases drastically (see Fig. 5). It should be noted that the profile of the  $2 \times 4$  spot depends solely on the remaining  $2 \times 4$  structure, which is described by a large  $2 \times 4$  domain with holes ( $\sqrt{3} \times \sqrt{3}$  domains). It does not depend on the domain boundaries of the  $\sqrt{3} \times \sqrt{3}$  structure. Unfortunately, the  $2 \times 4$  spot profile could not be separated into a central spike and a shoulder quantitatively due to low intensity. The shoulder is best described by a diameter of 3%, which is definitely less than the starting diameter of the  $\sqrt{3} \times \sqrt{3}$  spots with 6% and close to the value at the end of the  $t^{1/2}$  dependence.

#### D. Temperature dependence of growth kinetics

For saturation coverage the growth has been studied for temperatures between 344 and 415 K. For all experiments, a new layer of about  $\Theta = 0.6$  has been deposited on a well-annealed  $2 \times 4$  structure and then heated to the respective growth temperature up to 90 min. Only for  $T = 358$  K the growth at 344 K had been continued at the higher temperature. In all cases a portion with  $t^{1/2}$  has been found, as shown in Fig. 2. The first two points are uncertain with respect to time scale due to the time required for heating up to the measuring temperature. The dependence is therefore given by

$$H = S(T)(t - t_0)^{-1/2},$$

with  $t_0$  the (unknown) starting point,  $H$  the full width at half maximum. To obtain a straight line, the inverse square of  $H$  is plotted in Fig. 6 versus the annealing time, so that the starting point is no longer relevant for the determination of the slope  $S$ . It is seen that all curves start with the  $t^{1/2}$  dependence and switch to a slope with a lower exponent after some time. To derive an activation energy, the initial values of the slope in Fig. 6 have been plotted on a log scale versus inverse temperature in Fig. 7. The experimental points fit to an exponential dependence with an activation energy of  $E_{act} = 0.52$  eV.

#### IV. DISCUSSION

The ordering kinetics at surfaces have been studied theoretically in many details.<sup>6-14</sup> Several experiments have been evaluated along those lines.<sup>15-18</sup> Generally the kinetics is described by

$$\langle L(t) \rangle = S(T)t^x,$$

with  $\langle L(t) \rangle$  the average domain size,  $S(T)$  the rate constant, and  $x$  an exponent, which depends on growth con-

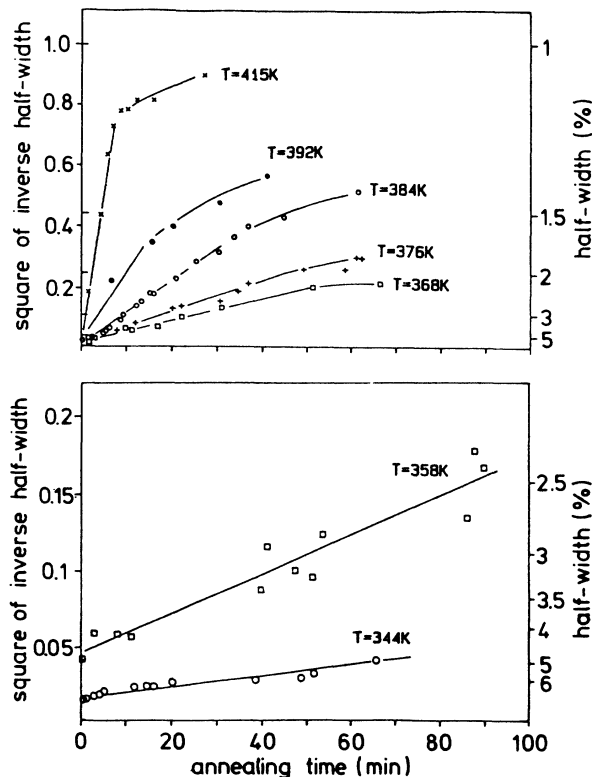


FIG. 6. Square of inverse half-width of  $\sqrt{3} \times \sqrt{3}$  superstructure spots vs annealing time for different annealing temperatures and saturation coverage of  $\sqrt{3} \times \sqrt{3}$  superstructure.

ditions like the degeneracy  $p$  of the growing domains and the possible equilibrium with the gas phase (constant versus variable coverage). For the present experiment constant coverage is given since evaporation of silver only starts at much higher temperatures. Whereas, for

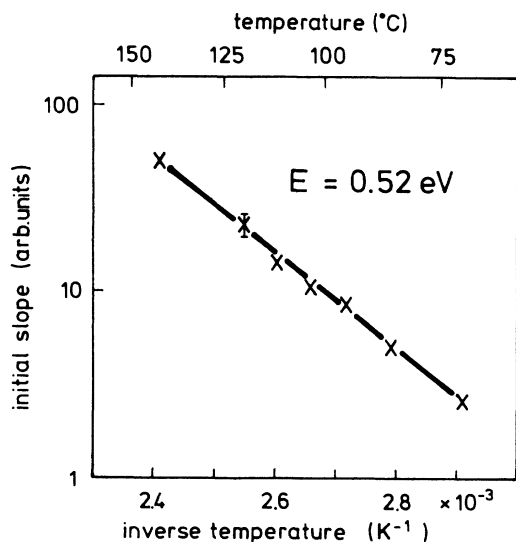


FIG. 7. Slope of the linear portions in Fig. 6 vs inverse temperature to reveal the activation energy for domain growth.

$p=2$  and nonconserved density, an exponent  $x=0.5$  is always predicted; it might be lower for  $p > 2$  and constant coverage. Since the structure grows in  $\sqrt{3} \times \sqrt{3}$  domains, the degeneracy  $p$  is at least 3. It may be larger since it grows on a perfect  $2 \times 4$  structure, which is converted into the  $\sqrt{3} \times \sqrt{3}$  structure in the newly formed patches. Therefore,  $p$  has to be within 3 and 24.

The average domain size is derived out of the spot profile of the extra spot, which is formed out of all the ordered domains. In the present case, both the well-ordered starting structure  $2 \times 4$  and the newly formed  $\sqrt{3} \times \sqrt{3}$  may be used. Since the  $2 \times 4$  superstructure forms a coherent structure, those spots consist of a central spike and a shoulder. The shoulder describes the parts not covered by  $2 \times 4$ , irrespective of the different  $\sqrt{3} \times \sqrt{3}$  domains. Since the  $\sqrt{3} \times \sqrt{3}$  domains nucleate at random (three translational domains, no rotational manifold), those extra spots consist of a shoulder without a central spike. Due to their intensity, the  $\sqrt{3} \times \sqrt{3}$  extra spots have been mainly used for measurement. The average domain size may be derived out of the half-width or the peak intensity. Their relation depends on spot profile. Since a Lorentzian profile has been found with high precision (Fig. 3), the domain-size distribution is geometric with the probability distribution  $P(n)=b(1-b)^{n-1}$  and  $1/b$  the average domain diameter. From the two-dimensional Lorentzian profile [ $I=I_0 a^3/(a^2+k^2)^{3/2}$ ] the half-width  $H$  (measured as FWHM) is inversely proportional to the average diameter  $\langle L \rangle$ ,

$$\langle L \rangle \approx 0.5/H,$$

where  $\langle L \rangle$  is measured in atomic distances and the  $H$  as a fraction of the next normal spot distance in the diffraction pattern. The approximate factor 0.5 is given by the geometric distribution [exactly  $(2^{2/3}-1)2/\pi$ ] and changes with the type of distribution. In the present experiment, therefore, the length  $\langle L \rangle$  is given as an absolute number. Frequently the peak intensity is used since it is more easily measured due to problems of exact measurements of the full profile down to the wings.<sup>16-18</sup> Even in cases where profiles were available, the evaluation has been based mainly on peak intensity.<sup>17</sup> The square root of the peak intensity is proportional to the average size  $\langle L \rangle$  only if the shape does scale exactly and if the integral intensity of the spot is constant during growth. So far these conditions have not been checked in former experiments. The scaling of the profile is demonstrated here in Fig. 3. It is also demonstrated in Fig. 4 that the integral intensity is only approximately constant, so that from the peak intensity, the exponent  $x$  would be determined too high. Here, therefore, only the half-width is used for evaluation. The difference is probably due to disordered Ag atoms at domain edges or boundaries, or as vacancies or interstitials in the domains, which modify peak intensities depending on the degree of order. For the quantitative evaluation of profiles, the contribution of the background has to be considered. Since thermal diffuse background and point defects are not to be included into domain-size distribution, the background has to be subtracted either by an extrapolation of the pair-correlation function<sup>26</sup> or by a numerical

fit of the sum of a Lorentzian and a constant, so that only the profile without a background is used for evaluation. In the present case, no subtraction was required since the intensity of the  $\sqrt{3} \times \sqrt{3}$  extra spots was so high that background subtraction had no effect on half-width or peak-intensity determination.

For annealing experiments, the period for heating up and cooling down may also be important, beside the annealing time at the top temperature. The analysis may therefore depend on the time intervals used for annealing. In the present experiments all measurements have been made at the temperature of annealing so that problems due to time intervals and heating cycles have been avoided completely except for the first heating up to the annealing temperature. Since the finite speed of heating up produces some uncertainty for the determination of the exact starting time, an evaluation procedure has been used which does not need an exact starting point, as described in Sec. III D.

The growth kinetics may be described either by moving of domain boundaries between adjacent domains or by diffusion of Ag atoms between well-separated islands. In the first case,  $x = \frac{1}{2}$ , is predicted<sup>7</sup> whereas for the second case,  $x = \frac{1}{3}$ , is expected.<sup>13</sup> For saturation coverage the first case should be dominant. If the activation energy  $E_{\text{meas}}$  of Fig. 7 is used to derive the activation energy of diffusion with  $\langle L \rangle \sim (Dt)^{1/2}$  and  $D = D_0 \exp(-E_{\text{diff}}/kT)$ , then  $E_{\text{diff}} = 1.04$  eV. This energy may be described by the barrier to rearrange a Ag atom at a domain boundary from the periodicity of the one domain to that of the other. Its value will depend heavily on the detailed

structure of the interface which is unknown so far. Therefore, it is difficult to speculate on that unexpected high value.

The growth of the larger domains (larger than 25 atomic distances) proceeds via a different mechanism. There might be blocking obstacles. A concentration of 1% would be sufficient. It has not been checked yet if this limiting value is influenced by sample treatment, so the model of obstacles is still speculative.

For lower coverages the domain-growth mode stops earlier. Very low coverages (less than 0.3), where percolation can be ruled out, have not yet been studied, so that a first growth via domain-wall movement has to be assumed. The second part may be due to island growth. Since a similar slowing down is found for saturation coverage, clear conclusions are not yet possible in this respect. The growth mode, however, with  $x = 0.5 \pm 0.05$ , is established for the first time by using the half-width in addition to the peak intensity, which is more relevant due to the constancy of spot shape.

Such measurements have been possible only with the high-resolution LEED system. It will be interesting to see if theory can provide the parameters necessary for the  $x = \frac{1}{2}$  dependence.

#### ACKNOWLEDGMENTS

The investigation has been supported by the Deutsche Forschungsgemeinschaft (Bonn, Germany). Helpful discussions with M. G. Lagally, H. U. Everts, K. Binder, and W. Moritz are gratefully acknowledged.

<sup>1</sup>Proceedings of the International Conference on the Formation of Semiconductor Interfaces, edited by G. Le Lay, D. Derrien, and C. A. Sebenne [Surf. Sci. **168** (1986)].

<sup>2</sup>Proceedings of the 2nd International Conference on the Formation of Semiconductor Interfaces, edited by A. Hiraki [Appl. Surf. Sci. **41/42** (1989)].

<sup>3</sup>J. J. Lander, Surf. Sci. **1**, 1 (1964).

<sup>4</sup>G. Binnig and H. Rohrer, Surf. Sci. **126**, 236 (1983).

<sup>5</sup>W. Teliens and E. Bauer, in *Structure of Surfaces II*, edited by J. E. van der Veen and M. A. Van Hove (Springer, Berlin, 1988), p. 53.

<sup>6</sup>I. M. Lifshitz, Zh. Eksp. Teor. Fiz. **42**, 1354 (1962) [Sov. Phys.—JETP **15**, 939 (1962)].

<sup>7</sup>S. M. Allen and J. W. Cahn, Acta Metall. **21**, 1085 (1979).

<sup>8</sup>K. Binder and D. Stauffer, Phys. Rev. Lett. **33**, 1006 (1974); K. Binder, Phys. Rev. B **15**, 4425 (1977).

<sup>9</sup>P. S. Sahni, D. J. Srolovitz, G. S. Grest, M. P. Anderson, and S. A. Safran, Phys. Rev. B **28**, 2705 (1983).

<sup>10</sup>J. D. Gunton, M. San Miquel, and P. S. Sahni, in *Phase Transitions and Critical Phenomena*, edited by C. Domb and J. L. Lebowitz (Academic, New York, 1983), Vol. 8.

<sup>11</sup>G. F. Mazenko and O. T. Valls, Phys. Rev. B **30**, 6732 (1984); F. C. Zhang, O. T. Valls, and G. F. Mazenko, *ibid.* **31**, 1579 (1985).

<sup>12</sup>A. Sadiq and K. Binder, J. Stat. Phys. **35**, 617 (1984).

<sup>13</sup>O. M. Lifshitz and V. V. Slyozov, J. Chem. Phys. Solids **15**, 35 (1961).

<sup>14</sup>P. S. Sahni and J. D. Gunton, Phys. Rev. Lett. **47**, 1754 (1981).

<sup>15</sup>M. C. Tringides, P. K. Wu, W. Moritz, and M. G. Lagally, Ber. Bunsenges. Phys. Chem. **90**, 277 (1986).

<sup>16</sup>G.-C. Wang and T.-M. Lu, Phys. Rev. B **31**, 5918 (1985).

<sup>17</sup>J.-K. Zuo, G.-C. Wang, and T.-M. Lu, Phys. Rev. Lett. **60**, 1053 (1988).

<sup>18</sup>P. K. Wu, M. C. Tringides, and M. G. Lagally, Phys. Rev. B (in press).

<sup>19</sup>M. Horn-von Hoegen, J. Falta, and M. Henzler, in Proceedings of the European Materials Research Society Conference, Strasbourg, 1989 [Thin Solid Films **182** (1989)].

<sup>20</sup>E. Suliga and M. Henzler, J. Vac. Sci. Tech. **A1**, 1507 (1983).

<sup>21</sup>E. Suliga and M. Henzler, J. Phys. C **16**, 1543 (1983).

<sup>22</sup>U. Scheithauer, G. Meyer, and M. Henzler, Surf. Sci. **178**, 441 (1986).

<sup>23</sup>R. Altsinger, H. Busch, M. Horn, and M. Henzler, Surf. Sci. **200**, 235 (1988).

<sup>24</sup>M. Hanbücken, T. Doust, O. Osasona, G. Le Lay, and J. A. Venables, Surf. Sci. **168**, 133 (1986).

<sup>25</sup>S. Tosch and H. Neddermeyer, Phys. Rev. Lett. **61**, 349 (1988).

<sup>26</sup>H. Busch and M. Henzler, Surf. Sci. **167**, 534 (1986).